Effect of DNA Flanking Sequence on Charge Transport in Short DNA Duplexes†

Xi Li, Yinghua Peng, Jinsong Ren, and Xiaogang Qu*

Division of Biological Inorganic Chemistry, Key Laboratory of Rare Earth Chemistry and Physics, Graduate School of the Chinese Academy of Sciences, Changchun Institute of Applied Chemistry, Chinese Academy of Sciences, Changchun, Jilin 130022, China

Received June 2, 2006; Revised Manuscript Received September 4, 2006

ABSTRACT: Several factors can influence charge transport (CT)-mediated DNA, such as sequence, distance, base stacking, base pair mismatch, conformation, tether length, etc. However, the DNA context effect or how flanking sequences influence redox active drugs in the DNA CT reaction and later in DNA enzymatic repair and synthesis is still not well understood. The set of seven DNA molecules in this study have been characterized well for the study of flanking sequence effects. These DNA duplexes are formed from self-complementary strands and contain the common central four-base sequence 5′-A-G-C-T-3′, flanked on both sides by either $(AT)_n$ or $(AA)_n$ ($n = 2$, 3, or 4) or $AA(AT)_2$. UV−vis, fluorescence, UV melting, circular dichroism, and cyclic voltammetry experiments were used to study the flanking sequence effect on CT-mediated DNA by using daunomycin or adriamycin cross-linked with these seven DNA molecules. Our results showed that charge transport was related to the flanking sequence, DNA melting free energy, and ionic strength. For $(AA)_n$ or $(AT)_n$ species of the same length, $(AA)_n$ series were more stable and more efficient CT was observed through the $(AA)_n$ series. The same trend was observed for $(AA)_n$ and $(AT)_n$ series at different ionic strengths, further supporting the idea that flanking sequence can result in different base stacking and modulate charge transport through these seven DNA molecules.

The dynamics and distance dependence of charge transport (CT) reactions proceeding through DNA may have important biological functions. Previous studies have shown that DNA damage and repair can result from the redox reactions of radicals with DNA, and these reactions are not only affected by the localized reaction but also modulated by the sequence and distance of charge transport-mediated DNA (*1*−*6*). Several mechanisms have been proposed for this long-range charge transport, such as multistep hopping (*7*−*10*), phonon-assisted polaron-like hopping (*11*−*13*), and coherent superexchange (*14*, *15*), which are all gated by dynamical variations within the stacking of π-electrons in DNA base pairs. The DNA π-stacking is capable of mediating oxidant DNA damage over long distances in a reaction, and this reaction is sensitive to sequence, distance, base stacking, base pair mismatch, conformation, tether length, etc. (*5*−*38*). It is well-known that the DNA flanking sequence context effect can greatly influence the base stacking and conformation (*39*−*42*). However, the DNA context effect or how flanking sequences influence redox active drugs in the DNA CT reaction and later in DNA enzymatic repair and synthesis is still not well understood. Seven DNA molecules we used in this study have been characterized well for the study of the flanking sequence effect (*39*). They are comprised of two 12-mers, three 14-mers, and two 20-mers (Figure 1). The seven molecules are formed from self-complementary strands and contain the common central four-base sequence 5′-A-G-C-T-3′ (Figure 2A), flanked on both sides by either $(AT)_n$ or $(AA)_n$ ($n = 2$, 3, or 4) or $AA(AT)_2$. Therefore, for the $(AT)_n$ and $(AA)_n$ series, the number of A·T (T·A) base pairs is the same and the only difference is the order of the A·T and T·A base pairs flanking the central drug specific binding site sequence (A-G-C-T). With this design, any differences in the nearest-neighbor contributions to long-range charge transport through DNA between any two duplexes of the same length should be attributable to differences in only flanking sequence contexts (*39*, *40*). Recently, we reported that DNA flanking sequence can cause enthalpy−entropy compensation when 7-aminoactinomycin D binds to these seven DNA molecules (*39*).

Various techniques and methods, including electrochemical probing, direct measurements of the electric conductivity of DNA (*43*, *44*), and spectral and biochemical techniques, have been employed in studying long-range DNA-mediated charge transport (*16*−*19*). In contrast to other techniques, the electrochemical method has advantages because of not only its distance, time, and energy regimes being distinct but also its measurement being conventional (*20*−*22*). Daunomycin (DM) and adriamycin (AM) (Figure 2B) are two widely used anthracycline anticancer antibiotics (*45*), and their cytotoxicities are enhanced by photoactivation (*46*). The reason for the enhanced effect induced by light can be related to previous results (*46*, *47*) which showed that the photoexcitation increases the rate of DM− and AM−DNA charge separation over that of the thermal reaction (barrier crossing) and triggers a redox cycling with a much higher efficiency,

† This work was supported by NSFC (Grants 20225102, 20331020, 20325101, and 20473084), the Fund from Jilin province, and the hundred people program from the Chinese Academy of Sciences.

* To whom correspondence should be addressed: Division of Biological Inorganic Chemistry, Key Laboratory of Rare Earth Chemistry and Physics, Changchun Institute of Applied Chemistry, Chinese Academy of Sciences, Changchun, Jilin 130022, China. Telephone: 86-431-526-2656. Fax: 86-431-5262656. E-mail: xqu@ciac.jl.cn.

10.1021/bi061103i CCC: $33.50
Published on Web 10/24/2006

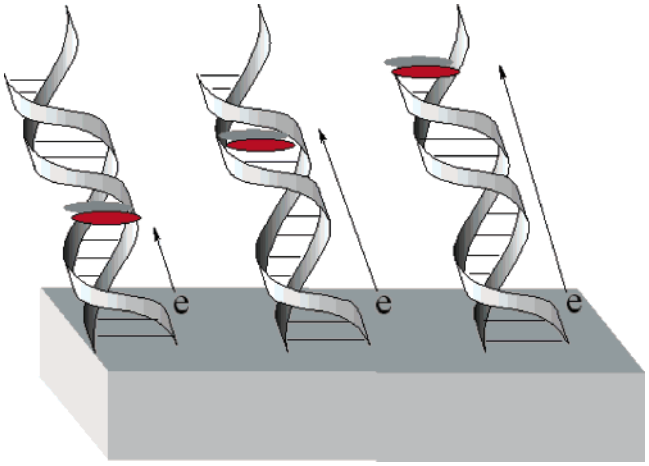

FIGURE 1: Schematic representation of DM or AM bound to different DNA-modified GCE electrodes (from left to right): 12-mer DNA, 16-mer DNA, and 20-mer DNA. DM or AM is colored red, and the likely paths of electron transfer are denoted with arrows.

thus resulting in enhanced cell killing by the anticancer drug (*46*). The reaction with oxygen guarantees the success of trajectories forming the superoxide. Since DM and AM have good electrochemical responses, they are widely used as probes to monitor the DNA-mediated CT process (*20*, *34*, *48*, *49*). In a typical electrochemical assay for DNA CT, a self-assembly DNA-modified electrode has been often used to examine charge transfer through DNA (*20*−*22*). Since the gold−thiol bond can withstand only reasonably mild potentials and the alkanethiols are prone to thermal desorption and oxidative damage, thiol−DNA molecules are easily oxidized in air, resulting in a gradual reduction in the level of DNA immobilization. It has been reported that DNA can strongly absorb on a glassy carbon electrode (GCE). The electrochemical behavior on a DNA-modified GCE (*50*) is similar to that on a gold electrode and can be used in a wider potential window. Furthermore, the electrochemical reversibility of the redox-active intercalator we used, daunomycin or adriamycin, is better on a GCE than on a Au electrode, and we chose a GCE as the working electrode in our experiments.

In this report, we employed UV−vis, fluorescence, UV melting, circular dichroism (CD), and cyclic voltammetry (CV) experiments in studying the flanking sequence effect on CT-mediated DNA by using DM and AM cross-linked (*51*−*53*) with these seven DNA molecules (Figure 1). Our results showed that charge transport was related to the flanking sequence, DNA melting free energy, and ionic strength. For $(AA)_n$ or $(AT)_n$ species of the same length, $(AA)_n$ series were more stable and more efficient CT was observed through $(AA)_n$ series. For $(AA)_n$ or $(AT)_n$ series, the longer the DNA chain, the slower the CT. The same trend was observed for $(AA)_n$ and $(AT)_n$ series at different ionic strengths, further supporting the idea that the flanking sequence can result in different base stacking and modulate charge transport through these seven DNA molecules.

MATERIALS AND METHODS

Materials. Daunomycin (DM, hydrochloride form) and adriamycin (AM, hydrochloride form) were purchased from Sigma and used without further purification. Ligand concentrations were estimated spectrophotometrically using an

A

DNA Sequence	Abbreviation
12mers	
5′-A-A-A-A-***A-G-C-T***-T-T-T-T-3′	$(AA)_2$
3′-T-T-T-T-***T-C-G-A***-A-A-A-A-5′	
5′-A-T-A-T-***A-G-C-T***-A-T-A-T-3′	$(AT)_2$
3′-T-A-T-A-***T-C-G-A***-T-A-T-A-5′	
16mers	
5′-A-A-A-A-A-A-***A-G-C-T***-T-T-T-T-T-T-3′	$(AA)_3$
3′-T-T-T-T-T-T-***T-C-G-A***-A-A-A-A-A-A-5′	
5′-A-T-A-T-A-T-***A-G-C-T***-A-T-A-T-A-T-3′	$(AT)_3$
3′-T-A-T-A-T-A-***T-C-G-A***-T-A-T-A-T-A-5′	
5′-A-A-A-T-A-T-***A-G-C-T***-A-T-A-T-T-T-3′	$(AA)(AT)_2$
3′-T-T-T-A-T-A-***T-C-G-A***-T-A-T-A-A-A-5′	
20mers	
5′-A-A-A-A-A-A-A-A-***A-G-C-T***-T-T-T-T-TT-T--T-3′	$(AA)_4$
3′-T-T-T-T-T-T-T-T-***T-C-G-A***-A-A-A-A-A-A-A-A-5′	
5′-A-T-A-T-A-T-A-T-A-T-***A-G-C-T***-A-T-A-T-A-T-A-T-A-T-3′	$(AT)_4$
3′-T-A-T-A-T-A-T-A-T-A-***T-C-G-A***-T-A-T-A-T-A-T-A-T-A-5′	

B

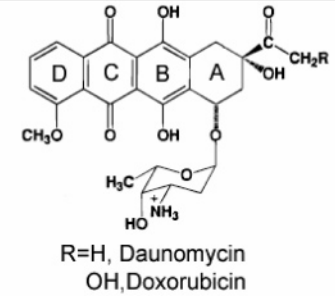

FIGURE 2: (A) Set of seven DNA oligomer duplexes that were studied. Bold italicized letters denote the primary binding site for daunomycin and adriamycin. The different 5′ flanking sequences are denoted at the right. (B) Chemical structures of daunomycin and adriamycin.

ϵ of 11 500 mol L^{-1} cm^{-1} at 480 nm (*45*). The DNA oligomers were purchased from Sangon (Shanghai, China). These oligomers were self-complementary (*39*), and these duplexes were prepared by heating the oligomers to 90 °C for 5 min, slowly cooling them to room temperature, and then equilibrating them for 48 h at 4 °C before they were used. Strand concentrations of these oligomers were determined by measuring the absorbance at 260 nm after melting (*39*). All experiments were carried out in aqueous Tris buffer [50 mM Tris and 100 mM NaCl (pH 7.1)] unless noted otherwise.

UV−Vis and Fluorescence Measurements. Absorbance measurements and melting studies were carried out on a JASCO V-550 UV−vis spectrophotometer, equipped with a Peltier temperature control accessory (*54*, *55*). Fluorescence spectra were measured on a JASCO FP-6500 spectrofluorometer equipped with a temperature-controlled water bath (*54*). All the spectra were recorded in a 1.0 cm path length cell with Tris buffer as the reference solution. Absorbance changes at 260 nm versus temperature were collected at a heating rate of 0.5 °C/min, over the temperature range of

10−96 °C. DNA strand concentrations were ~3.0 μM in Tris buffer. Primary data were transferred to Origin for plotting and analysis. With the widely used method (*56*), the thermodynamic parameters of these seven short oligomer DNA duplexes were calculated through their melting profiles.

CD Spectral Measurements. A JASCO J-810 circular dichroism spectropolarimeter was used for CD spectral measurements (*54*, *55*) using a quartz cell with a path length of 0.5 cm. The optical chamber of the CD spectrometer was deoxygenated with dry purified nitrogen (99.99%) for 45 min before use, and the nitrogen atmosphere was maintained during experiments. The temperature in the sample compartment was kept at 20 °C during the experiment. All CD spectra of sample solutions recorded here were the CD spectra with the background subtracted. The final spectrum was obtained by automatic averaging over three consecutive scans.

Electrochemistry Measurements. Cyclic voltammetry (CV) was carried out with a CHI660B electrochemistry workstation (CHI). All electrochemical experiments (*57*, *58*) employed a conventional three-electrode cell (1 mL, single electrolyte compartment) with a glass carbon electrode (CHI) used as the working electrode, a platinum wire as the auxiliary electrode, and a Ag/AgCl electrode (saturated KCl solution) as the reference electrode. The cell was thermostated at 20 ± 1 °C. The buffer was purged with purified nitrogen (99.99%) for more than 20 min prior to a series of experiments.

Cross-Linking of DM or AM with DNA. The cross-linking of DM or AM with DNA was carried out as described previously (*51*). Briefly, each DNA duplex containing an adjacent pair of guanine residues was hybridized (*39*), incubated with 0.003% formaldehyde and DM or AM in Tris buffer for 1 h, and extracted with phenol. Subsequently, the samples were dialyzed (*45*) against Tris buffer for 24 h to remove the phenol.

Modification of the Glass Carbon Electrode. The glass carbon electrode (Φ = 3.0 cm, CHI) was polished successively with 1.0, 0.3, and 0.05 μm alumina (Buhler) and sonicated for 5 min (*57*, *58*). The GCE was then transferred into a DM cross-linked DNA solution in Tris buffer and held for 12 h at 4 °C. After that, the modified electrode was taken out and rinsed with water prior to use. Control experiments were carried out on the bare and DNA-modified GCE.

RESULTS AND DISCUSSION

UV Melting. Figure 3 shows the UV melting profiles of DNA alone (part A) and 1:1 covalently DM cross-linked DNA complexes (part B). The DNA molecules were 12-mer $(AA)_2$ and $(AT)_2$ series. Similar results were obtained for AM (data not shown). It was obvious that the DNA with the $(AA)_2$ flanking sequence (black curve) was more stable than that with the $(AT)_2$ flanking sequence (red curve), consistent with our previous report (*39*). The difference in melting temperature (T_m) between two duplexes was ~3 °C. Table 1 summarized the melting temperatures and their thermodynamic parameters for these seven DNA molecules. For $(AA)_n$ and $(AT)_n$ series of the same length, $(AA)_n$ DNA was more stable than $(AT)_n$ DNA and the melting temperature of the $(AA)(AT)_2$ hybrid DNA molecule was intermediate between those of $(AA)_3$ and $(AT)_3$ molecules (*39*).

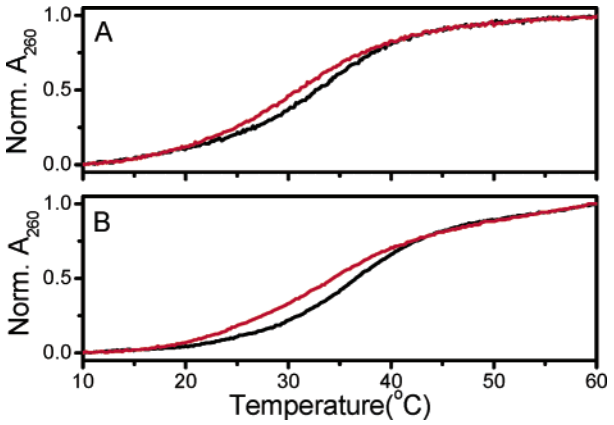

FIGURE 3: DNA UV melting profiles of duplex $(AA)_2AGCT(TT)_2$ (black curves) and $(AT)_2AGCT(TA)_2$ (red curves) in Tris buffer [50 mM Tris and 100 mM NaCl (pH 7.1)]: (A) DNA alone and (B) DNA with DM cross-linked. The details are given in Materials and Methods.

Table 1: Thermodynamic Parameters for Duplex DNAs[a]

DNA	T_m^0 (°C)	T_m (°C)	ΔT (°C)	ΔH (kJ/mol)	ΔS (J mol^{-1} K^{-1})	ΔG_{20} (kJ/mol)
$(AA)_2$	33.0	35.5	2.5	−197.2	−534.2	−40.7
$(AT)_2$	30.0	33.0	3.0	−189.4	−513.6	−38.9
$(AA)_3$	42.5	45.5	3.0	−226.8	−608.7	−48.5
$(AT)_3$	39.0	44.5	5.5	−194.0	−512.4	−43.9
$(AA)(AT)_2$	39.0	43.0	4.0	−211.7	−569.2	−45.0
$(AA)_4$	49.0	53.0	4.0	−239.3	−632.4	−54.0
$(AT)_4$	44.5	51.0	6.5	−206.0	−540.7	−47.6

[a] The thermodynamic parameters of DNA alone were calculated according to the method in ref *51*. The enthalpy change, ΔH, was determined from the temperature dependence of the equilibrium association constant where ΔH was the slope of the ln K_a vs $1/T$ plot according to the equation $\ln K_a = -(\Delta H/RT) + \Delta S/R$, where ΔS is the entropy change that was calculated according to the *Y*-axis intercept. The free energy change (ΔG) at 20 °C was calculated from the standard Gibbss equation ($\Delta G = \Delta H - T\Delta S$), and the errors were within 15%. Total strand concentrations were ~3 μM. $\Delta T = T_m - T_m^0$; T_m and T_m^0 represent the melting temperature of DNA alone and cross-linked with DM in Tris buffer [50 mM Tris and 100 mM NaCl (pH 7.1)], respectively.

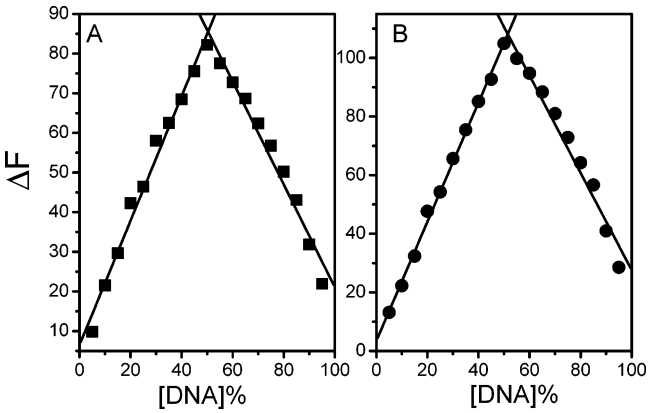

FIGURE 4: Job plots of daunomycin bound to $(AA)_2$ DNA (A) and $(AT)_2$ DNA (B). The total concentration of daunomycin and DNA was held constant at 60 μM over the course of the titration. The excitation wavelength was 480 nm. The fluorescence difference at 555 nm ($F_{drug} - F_{drug-DNA}$) was plotted vs the percentage of DNA.

As shown in Table 1, for $(AA)_2$ DNA, the free energy change at room temperature (ΔG_{20}) was −40.7 ± 0.1 kJ/mol, more favorable than that for $(AT)_2$ DNA with a $\Delta\Delta G_{20}$ of approximately −1.8 kJ/mol. The more favorable free

Table 2: Parameters for Daunomycin−DNA Binding[a]

	$(AA)_2$	$(AT)_2$	$(AA)_3$	$(AT)_3$	$(AA)(AT)_2$	$(AA)_4$	$(AT)_4$
N (duplex)	1.0	1.0	1.0	1.0	1.0	1.0	1.0
K [(M duplex)$^{-1}$]	4.6×10^5	3.8×10^6	3.6×10^6	7.6×10^6	5.7×10^6	4.2×10^6	9.1×10^6

[a] *N* is the binding stoichiometry determined by the continuous variation method. *K* was the binding constant which was determined by fluorescence titration (*63*). Fixed drug concentrations were titrated with increasing DNA concentrations in Tris buffer. Fluorescence titration data (*63*) were fit directly to obtain binding constants, using a fitting function incorporated into FitAll (MTR Software, Toronto, ON). Errors in the binding parameters resulting from the fitting procedure were <15%.

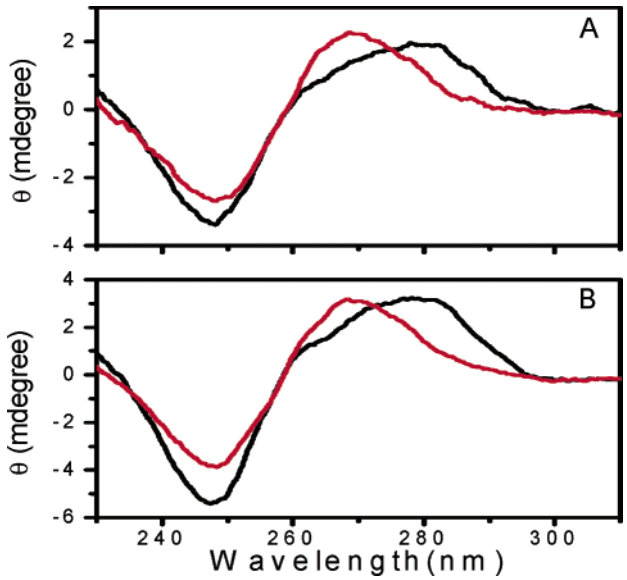

FIGURE 5: (A) Circular dichroism spectra of $(AA)_2AGCT(TT)_2$ (black) and $(AT)_2AGCT(TA)_2$ duplex DNA (red) measured in Tris buffer [50 mM Tris and 100 mM NaCl (pH 7.1)]. (B) Circular dichroism spectra of DM-cross-linked $(AA)_2AGCT(TT)_2$ (black) and $(AT)_2AGCT(TA)_2$ DNA (red) in the same solution as in panel A.

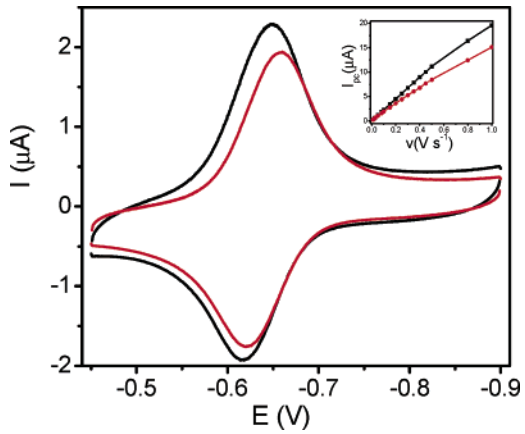

FIGURE 6: Cyclic voltammograms of DM cross-linked with $(AA)_2AGCT(TT)_2$ (black) and $(AT)_2AGCT(TA)_2$ duplex DNA (red) on a modified GCE at a scan rate of 100 mV/s in Tris buffer [50 mM Tris and 100 mM NaCl (pH 7.1)]. The inset shows plots of I_{pc} for DM cross-linked with $(AA)_2AGCT(TT)_2$ (black) and $(AT)_2AGCT(TA)_2$ duplex DNA (red) as a function of scan rate. The linear relationship showed that the electrochemical process was surface-controlled.

energy for $(AA)_2$ DNA was from a more favorable enthalpy ($\Delta\Delta H_{20} \sim -7.8$ kJ/mol) because its entropy was even less favorable than that of $(AT)_2$ DNA with a $\Delta\Delta S_{20}$ of ~20.6 J mol^{-1} K^{-1}. Similar results were observed for the DNAs flanked by longer $(AA)_n$ or $(AT)_n$ sequences, showing enthalpy−entropy compensation for these seven DNA molecules (*39*). With this design, the differences among these DNA molecules should be attributable to differences in only flanking sequence contexts, and different base stackings can make different contributions (*39*−*42*, *59*−*61*). We were aware that the thermodynamic data we reported here were different from previous data reported by Benight et al. (*62*). The difference might be due to the different buffer properties, the different ionic strengths, and the different determination methods (*62*). The earlier studies were performed in phosphate buffer and at different ionic strengths, while the studies presented here use Tris buffer. We chose Tris buffer because we shall further study the flanking sequence effect on the binding of drug to DNA in the presence of different kinds of metal ions.

For these seven $(AT)_n$ and $(AA)_n$ series DNA duplexes, all of them have one G·C base pair and can form a 1:1 covalent DM−DNA adduct by formaldehyde cross-linking of 3′-NH_2 anthracyclines to the N2 amine of guanine (*51*). When the DNA was cross-linked with DM (*20*, *51*), the DNA melting temperature (T_m) was increased. As shown in Figure 3 and Table 1, for the $(AA)_2$ fragments, the difference in T_m between DNA cross-linked with drug and DNA alone ($\Delta T = T_m - T_m^0$) was smaller than that of the $(AT)_2$ DNA. The same trend but with a larger ΔT was observed for the other series, showing that the stability of $(AT)_n$ series increased more rapidly than that of $(AA)_n$ series when DM bound. Similar results were obtained for DM bound to DNA without cross-linking (data not shown). These results showed that increasing the DNA stability via binding of DM was related to the flanking sequence, and the flanking sequence effect remained even if DM was cross-linked with DNA. In addition, the 1:1 binding stoichiometry for DM bound to these seven DNA molecules was confirmed by a continuous variation method (*54*); typical data for DM bound to $(AA)_2$ and $(AT)_2$ in solution are shown in Figure 4. DNA binding constants were determined by the fluorescence titration method (*63*) and are summarized in Table 2. The DNA binding constant was increased with an increase in the length of the flanking sequence. For the same length $(AA)_n$ or $(AT)_n$ series, DM bound stronger to $(AT)_n$ series that to $(AA)_n$ series, in accordance with the fact that the stability of $(AT)_n$ series increased more rapidly than that of the $(AA)_n$ series when DM bound (Table 1). This behavior was different from that for binding of 7-aminoactinomycin D to these DNA molecules (*39*), showing that the flanking sequence effect on drug bound to DNA was complicated, and related not only to DNA itself but also to drug property and solution conditions. This deserves further study.

Circular Dichroism Studies. These seven DNA molecules adopted a typical B-type structure. Figure 5A shows the CD spectra of $(AA)_2$ and $(AT)_2$ DNA. For $(AT)_n$ series, the maximum positive band was at 273 nm while it was red-

Table 3: Summary of the Electrochemical Parameters of 10 μM DM on a GCE and a GCE Modified with DNA in Tris Buffer [50 mM Tris and 100 mM NaCl (pH 7.1)][a]

electrode	E_c (mV)	E_a (mV)	i_{pc} (μA)	i_{pa} (μA)	$E^{\circ\prime}$ (mV)	ΔE (mV)
GCE	−655	−629	2.351	−2.197	−642.0	26
$(AA)_2$/GCE	−660	−629	1.336	−1.216	−644.5	31
$(AT)_2$/GCE	−658	−632	1.107	−1.187	−645.0	26
$(AA)_3$/GCE	−662	−631	0.6471	−0.6186	−646.5	31
$(AT)_3$/GCE	−660	−633	0.3675	−0.4368	−646.5	27
$(AA)(AT)_2$/GCE	−658	−635	0.3820	−0.4538	−646.5	23
$(AA)_4$/GCE	−660	−625	0.6038	−0.6099	−642.5	35
$(AT)_4$/GCE	−662	−623	0.3583	−0.4029	−642.5	39

[a] The errors in the electrochemical measurements were <10%. The scanning rate was 100 mV/s.

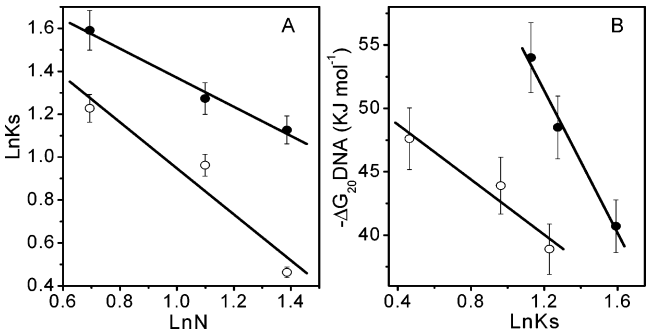

FIGURE 7: (A) Plots of ln K_s vs ln N (number of AA or AT pairs in DNA) for 10 μM DM measured in $(AA)_n$ series DNA (●) and $(AT)_n$ series DNA (○) on a modified GCE in Tris buffer [50 mM Tris and 100 mM NaCl (pH 7.1)]. The slope is −0.7 ($R = -0.99$) and −1.1 ($R = -0.96$) for $(AA)_n$ and $(AT)_n$ series DNA, respectively. (B) Relationship of DNA free energy [$-\Delta G_{20}$(DNA)] vs ln K_s for $(AA)_n$ series (●) and $(AT)_n$ series DNA (○) measured in Tris buffer [50 mM Tris and 100 mM NaCl (pH 7.1)]. DNA free energy [$-\Delta G_{20}$(DNA)] values were calculated from their melting profiles.

shifted to 278 nm for $(AA)_n$ series, and the hybrid $(AA)(AT)_2$ DNA spectra were similar to those of the $(AA)_n$ molecules, showing that base stackings were different for $(AA)_n$ and $(AT)_n$ series. DM cross-linking appeared not to alter significantly the DNA secondary structure (*39*). Subtle structural differences still existed for the DNA molecules (Figure 5B). Similar results were obtained for DM noncovalently bound to these seven DNA molecules (data not shown), consistent with the UV melting results. Therefore, cross-linking of DM with $(AA)_n$ or $(AT)_n$ series may be applied in studying the effect of the flanking sequence on DNA-mediated charge transport since DM was fixed to the binding site and flanking sequence effects remained.

Transport of Charge through DNA. Besides daunomycin and adriamycin as common electrochemical probes which can be cross-linked to DNA to study charge transport-mediated DNA, they are frequently used in the clinic, and previous studies have shown that they have a preference for the G·C base pair (*45*) and their actions involved redox reactions (*46*, *47*). Interestingly, upon photoactivation, the cell killing efficiency was greatly enhanced (*46*, *47*). Therefore, we selected daunomycin and adriamycin to study the effect of flanking sequence on the transport of charge through DNA. Irrespective of flanking sequence, DM exhibited an electrochemically reversible reduction of ca. −644 mV versus Ag/AgCl-saturated KCl on an all DNA-modified glassy carbon electrode (GCE) which was attributed to the anthraquinone groups being reduced to the dihydroxyl anthraquinone corresponding to a $2e^-/2H^+$ process (Figure 6) (*64*). However, the current intensity was dependent on the flanking sequence; i.e., for the same series $(AA)_n$ or $(AT)_n$ DNA, the longer the DNA chain, the weaker the observed peak current; for the same length $(AA)_n$ and $(AT)_n$ series, the peak currents of the DM−$(AA)_n$ adducts were stronger than those of DM cross-linked with the $(AT)_n$ DNA and the peak currents of the $(AA)(AT)_2$ hybrid DNA molecule were intermediate between those of the $(AA)_3$ and $(AT)_3$ molecules (Table 3), consistent with UV melting and CD studies.

Due to the peak currents being proportional to the scan rate, the electrochemical process of DM and DNA−DM complexes on GCE was surface-controlled (Figure 6, inset) (*65*). Plots of the difference in cathodic and anodic peak separation (ΔE_{pc} and ΔE_{pa}, respectively) as a function of scan rate according to Laviron's model yielded standard electron transfer rate constants, K_s, for $(AA)_n$ and $(AT)_n$ series (*66*). Figure 7A shows that the relationship between ln K_s and the number of AA or AT pairs. The transport of charge through the $(AA)_n$ series DNA was faster than that through the $(AT)_n$ series, and the rate was correlated with the DNA free energy (Figure 7B). For the same series $(AA)_n$ or $(AT)_n$ DNA, DNA became more stable with an increase in the length of the flanking sequence while the CT rate became slower. For the same length $(AA)_n$ and $(AT)_n$ series, $(AA)_n$ species were more stable, but the charge transport became more efficient, further indicating that the flanking sequence could affect the base stacking of DNA, thereby modulating the charge transport. Recent studies have shown the tether length of the alkane linker for the DNA chain strongly influences the charge transport rate (*34*). As CT through alkane chains is considerably slower than CT through DNA chains, the decrease in the CT rate constant with an increase in the number of CH_2 units is sharper than that with the increase in the number of AA or AT pairs (*67*).

In addition, we measured the electrochemical property of DM covalently and noncovalently bound to DNA in solution at a bare GCE and obtained results similar to those of the case with a DNA-modified GCE surface (Tables 4 and 5) (*68*); i.e., for $(AA)_n$ and $(AT)_n$ series, the charge transport was more efficient through the $(AA)_n$ series. DM covalently or noncovalently bound to DNA did not have exert much difference on the CT through these seven DNA molecules, showing that the DNA flanking sequence could modulate the DNA-mediated CT process both on the modified electrode surface and in solution.

Ionic Strength Dependence of the Transfer of Charge through DNA. Ionic strength was found to play an important role in charge transport-mediated DNA in solution. Figure 8 shows that the K_s decreased with an increase in the ionic

Table 4: Summary of the Electrochemical Parameters of 1 μM Cross-Linked DM with DNA on a GCE in Tris Buffer [50 mM Tris and 100 mM NaCl (pH 7.1)][a]

electrolyte	E_c (mV)	E_a (mV)	i_{pc} (μA)	i_{pa} (μA)	$E^{\circ\prime}$ (mV)	ΔE (mV)
DM−$(AA)_2$	−643	−625	0.4614	−0.4865	−634.0	18
DM−$(AT)_2$	−643	−621	0.4232	−0.4541	−632.0	22
DM−$(AA)_3$	−647	−626	0.3361	−0.3506	−636.5	21
DM−$(AT)_3$	−647	−628	0.2786	−0.2983	−637.5	19
DM−(AA)$(AT)_2$	−648	−624	0.3781	−0.3373	−636.0	24
DM−$(AA)_4$	−647	−628	0.2413	−0.2743	−637.5	19
DM−$(AT)_4$	−644	−623	0.2084	−0.2282	−633.5	21

[a] The errors in the electrochemical measurements were <10%. The scanning rate was 100 mV/s.

Table 5: Summary of the Electrochemical Parameters of 1 μM DM without and with 1 μM DNA on a GCE in Tris Buffer [50 mM Tris and 100 mM NaCl (pH 7.1)][a]

electrolyte	E_c (mV)	E_a (mV)	i_{pc} (μA)	i_{pa} (μA)	$E^{\circ\prime}$ (mV)	ΔE (mV)
DM	−651	−629	1.419	1.452	−640.0	22
DM−$(AA)_2$	−652	−625	0.8324	−0.8685	−638.5	27
DM−$(AT)_2$	−654	−624	0.8289	−0.8478	−639.0	30
DM−$(AA)_3$	−641	−620	0.7698	−0.7541	−630.5	21
DM−$(AT)_3$	−649	−622	0.6561	−0.6596	−635.5	27
DM−(AA)$(AT)_2$	−648	−623	0.7374	−0.7123	−635.5	25
DM−$(AA)_4$	−648	−628	0.6049	−0.6491	−638.0	20
DM−$(AT)_4$	−648	−621	0.5034	−0.5433	−634.5	27

[a] The errors in the electrochemical measurements were <10%. The scanning rate was 100 mV/s.

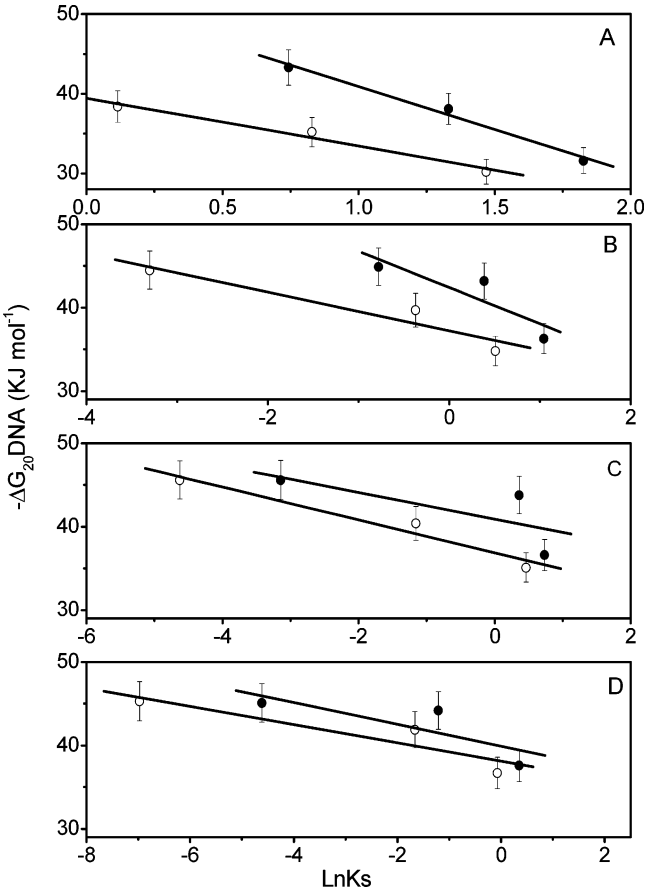

FIGURE 8: Relationship of DNA free energy [$-\Delta G_{20}$(DNA)] vs ln K_s for noncovalently bound complex DM−$(AA)_n$ series (●) and DM−$(AT)_n$ series DNA (○) measured in Tris buffer [50 mM Tris (pH 7.1)] at different NaCl concentrations: (A) 100, (B) 200, (C) 300, and (D) 400 mM.

strength, consistent with the relationship between DNA free energy and K_s. The exact mechanism is not clear; however, several factors may impact the transfer of charge through the DNA chain when ionic strength increases. (i) A high ionic strength increases DNA stability which would make dynamical variations within the stacking of π-electrons in DNA base pairs more difficult (*7*−*15*) and results in decreased K_s values, further supporting the idea that K_s depends on DNA free energy. (ii) Since the amino group in DM was protonated at pH 7.0 and binding of DM to DNA would release sodium ions, DM binding affinity would decrease at higher NaCl concentrations, causing the decrease in currents in the cyclic voltammograms. (iii) Chloride ions would exclude polyanionic DNA from the electrode surface which would slow the transfer of charge through DNA. The chloride exclusion effect may play major role at higher ionic strengths, such as at 0.4 M NaCl. There is a modest effect on stability going from $(AT)_2$ to $(AT)_3$ and almost no effect going from $(AA)_2$ to $(AA)_3$; however, there were substantial decreases in the rate of charge transfer. This may be due to the chloride exclusion effect. As shown in Figure 8A at 100 mM NaCl, the difference in base stacking between $(AA)_n$ or $(AT)_n$ series remained. Although the K_s for DM−DNA complex decreased with the ionic strength increase, the trend for CT did not change with ionic strength; therefore, the difference should be attributable to differences in only flanking sequence contexts, as we previously reported that the DNA flanking sequence can cause enthalpy and/or entropy compensation when 7-aminoactinomycin D binds to these seven DNA molecules (*39*).

CONCLUSIONS

The effect of DNA flanking sequence on charge transport was studied using these seven well-characterized $(AA)_n$ and $(AT)_n$ series DNA molecules. It can be concluded that (i) for $(AA)_n$ or $(AT)_n$ series, the CT rate was related to the DNA free energy and K_s was decreased with an increase in the length of the flanking sequence; (ii) for the same length $(AA)_n$ and $(AT)_n$ series, charge transport was more efficient through $(AA)_n$ series which should be attributed to the subtle difference in base stacking among these DNA molecules;

and (iii) K_s decreases with an increase in ionic strength.

ACKNOWLEDGMENT

We thank Dr. A. S. Benight for his help on the flanking sequence project. We are grateful for the referees' helpful comments on the manuscript.

REFERENCES

1. Szent-Györgi, A., Isenberg, I., and Baird, S. J., Jr. (1960) On the electron donating properties of carcinogens, *Proc. Natl. Acad. Sci. U.S.A. 46*, 1444−1449.
2. Fink, H. W., and Schonenberger, C. (1999) Electrical conduction through DNA molecules, *Nature 398*, 407−410.
3. Wan, C., Fiebig, T., Kelley, S. O., Treadway, C. R., Barton, J., and Zewail, A. H. (2000) Femtosecond dynamics of DNA-mediated electron transfer, *Proc. Natl. Acad. Sci. U.S.A. 97*, 14052−14055.
4. DeRosa, M. C., Sancar, A., and Barton, J. K. (2005) Electrically monitoring DNA repair by photolyase, *Proc. Natl. Acad. Sci. U.S.A. 102*, 10788−10792.
5. Hall, D. B., Holmlin, R. E., and Barton, J. K. (1996) Oxidative DNA damage through long-range electron transfer, *Nature 382*, 731−735.
6. Boon, E. M., Livingston, A. L., Chmiel, N. H., Davis, S. S., and Barton, J. K. (2003) DNA-mediated charge transport for DNA repair, *Proc. Natl. Acad. Sci. U.S.A. 100*, 12543−12547.
7. Meggers, E., Michel-Beyerle, M. E., and Giese, B. (1998) Sequence dependent long range hole transport in DNA, *J. Am. Chem. Soc. 120*, 12950−12955.
8. Giese, B. (2000) Long distance charge transport in DNA: The hopping mechanism, *Acc. Chem. Res. 33*, 631−636.
9. Giese, B., Amaudrut, J., Kohler, A. K., Spormann, M., and Wessely, S. (2001) Direct observation of hole transfer through DNA by hopping between adenine bases and by tunnelling, *Nature 412*, 318−320.
10. Bixon, M., Giese, B., Wessely, S., Langenbancher, T., Michel-Beyerle, M. E., and Jortner, J. (1999) Long-range charge hopping in DNA, *Proc. Natl. Acad. Sci. U.S.A. 96*, 11713−11716.
11. Schuster, G. B. (2000) Long-range charge transfer in DNA: Transient structural distortions control the distance dependence, *Acc. Chem. Res. 33*, 253−260.
12. Henderson, P. T., Jones, D., Hampikian, G., Kan, Y. Z., and Schuster, G. B. (1999) Long-distance charge transport in duplex DNA: The phonon-assisted polaron-like hopping mechanism, *Proc. Natl. Acad. Sci. U.S.A. 96*, 8353−8358.
13. Ly, D., Kan, Y. Z., and Schuster, G. B. (1999) Mechanism of charge transport in DNA: Internally-linked anthraquinone conjugates support phonon-assisted polaron hopping, *J. Am. Chem. Soc. 121*, 9400−9410.
14. Lewis, F. D., Letsinger, R. L., and Wasielewski, M. R. (2001) Dynamics of photoinduced charge transfer and hole transport in synthetic DNA hairpins, *Acc. Chem. Res. 34*, 159−170.
15. Lewis, F. D., Wu, T. F., Liu, X. Y., Letsinger, R. L., Greenfield, S. R., Miller, S. E., and Wasielewski, M. R. (2000) Dynamics of photoinduced charge separation and charge recombination in synthetic DNA hairpins with stilbenedicarboxamide linkers, *J. Am. Chem. Soc. 122*, 2889−2902.
16. O'Neill, M. A., and Barton, J. K. (2004) DNA-mediated charge transport chemistry and biology, *Top. Curr. Chem. 236*, 67−115.
17. Erkkila, K. E., Odom, D. T., and Barton, J. K. (1999) Recognition and reaction of metallointercalators with DNA, *Chem. Rev. 99*, 2777−2795.
18. Arkin, M. R., Stemp, E. D. A., Holmlin, R. E., Barton, J. K., Hormann, A., Olson, E. J. C., and Barbara, P. F. (1996) Rates of DNA-mediated electron transfer between metallointercalators, *Science 273*, 475−480.
19. Kelley, S. O., and Barton, J. K. (1999) Electron transfer between bases in double helical DNA, *Science 283*, 375−381.
20. Kelley, S. O., Jackson, N. M., Hill, M. G., and Barton, J. K. (1999) Long-range electron transfer through DNA films, *Angew. Chem., Int. Ed. 38*, 941−945.
21. Jackson, N. M., and Hill, M. G. (2001) Electrochemistry at DNA-modified surfaces: New probes for charge transport through the double helix, *Curr. Opin. Chem. Biol. 5*, 209−215.
22. Kelley, S. O., Barton, J. K., Jackson, N. M., and Hill, M. G. (1997) Electrochemistry of methylene blue bound to a DNA-modified electrode, *Bioconjugate Chem. 8*, 31−37.
23. Lewis, F. D., Wu, T. F., Zhang, Y. F., Letsinger, R. L., Greenfield, S. R., and Wasielewski, M. R. (1997) Distance-dependent electron transfer in DNA hairpins, *Science 277*, 673−676.
24. Fukui, K., and Tanaka, K. (1998) Distance dependence of photoinduced electron transfer in DNA, *Angew. Chem., Int. Ed. 37*, 158−161.
25. Sugiyama, H., and Saito, I. (1996) Theoretical studies of GC-specific photocleavage of DNA via electron transfer: Significant lowering of ionization potential and 5′-localization of HOMO of stacked GG bases in B-form DNA, *J. Am. Chem. Soc. 118*, 7063−7068.
26. Meade, T. J., and Kayyem, J. F. (1995) Electron-transfer through DNA site-specific modification of duplex DNA with ruthenium donors and accepters, *Angew. Chem., Int. Ed. 34*, 352−354.
27. Holmlin, R. E., Dandliker, P. J., and Barton, J. K. (1997) Charge transfer through the DNA base stack, *Angew. Chem., Int. Ed. 36*, 2715−2730.
28. Kelly, S. O., and Barton, J. K. (1998) DNA-mediated electron transfer from a modified base to ethidium: π-stacking as a modulator of reactivity, *Chem. Biol. 5*, 413−425.
29. Hall, D. B., and Barton, J. K. (1997) Sensitivity of DNA-mediated electron transfer to the intervening π-stack: A probe for the integrity of the DNA base stack, *J. Am. Chem. Soc. 119*, 5045−5046.
30. Dandliker, P. J., Holmlin, R. E., and Barton, J. K. (1997) Oxidative thymine dimer repair in the DNA helix, *Science 275*, 1465−1468.
31. Boon, E. M., and Barton, J. K. (2003) DNA electrochemistry as a probe of base pair stacking in A-, B-, and Z-form DNA, *Bioconjugate Chem. 14*, 1140−1147.
32. Lewis, F. D., Zhang, Y. F., Liu, X. Y., Xu, N., and Letsinger, R. L. (1999) Naphthalenedicarboxamides as fluorescent probes of inter- and intramolecular electron transfer in single strand, hairpin, and duplex DNA, *J. Phys. Chem. B 103*, 2570−2578.
33. Holmberg, R. C., and Thorp, H. H. (2004) Electrochemical determination of triple helices: Electrocatalytic oxidation of guanine in an intramolecular triplex, *Inorg. Chem. 43*, 5080−5085.
34. Drummond, T. G., Hill, M. G., and Barton, J. K. (2004) Electron transfer rates in DNA films as a function of tether length, *J. Am. Chem. Soc. 126*, 15010−15011.
35. Kelly, S. O., Holmlin, R. E., Stemp, E. D. A., and Barton, J. K. (1997) Photoinduced electron transfer in ethidium-modified DNA duplexes: Dependence on distance and base stacking, *J. Am. Chem. Soc. 119*, 9861−9870.
36. Holmlin, R. E., Tong, R. T., and Barton, J. K. (1998) Long-range triplet energy transfer between metallointercalators tethered to DNA: Importance of intercalation, stacking, and distance, *J. Am. Chem. Soc. 120*, 9724−9725.
37. Kelley, S. O., Boon, E. M., Barton, J. K., Jackson, N. M., and Hill, M. G. (1999) Single-base mismatch detection based on charge transduction through DNA, *Nucleic Acids Res. 27*, 4830−4837.
38. Boon, E. M., Jackson, N. M., Wightman, M. D., Kelley, S. O., Hill, M. G., and Barton, J. K. (2003) Intercalative Stacking: A Critical Feature of DNA Charge-Transport Electrochemistry, *J. Phys. Chem. B 107*, 11805−11812.
39. Qu, X. G., Ren, J. S., Riccell, P. V., Benight, A. S., and Chaires, J. B. (2003) Enthalpy/Entropy Compensation: Influence of DNA Flanking Sequence on the Binding of 7-Amino Actinomycin D to Its Primary Binding Site in Short DNA Duplexes, *Biochemistry 42*, 11960−11967.
40. Riccelli, P. V., Vallone, P. M., Kashin, I., Faldasz, B. D., Lane, M. J., and Benight, A. S. (1999) Thermodynamic, spectroscopic, and equilibrium binding studies of DNA sequence context effects in six 22-base pair deoxyoligonucleotides, *Biochemistry 38*, 11197−11208.
41. Fredrik Edfeldt, N. B., Harwood, E. A., Sigurdsson, S. T., Hopkins, P. B., and Reid, B. R. (2004) Sequence context effect on the structure of nitrous acid induced DNA interstrand cross-links, *Nucleic Acids Res. 32*, 2795−2801.
42. Lindqvist, M., and Graslund, A. (2001) An FTIR and CD study of the structural effects of G-tract length and sequence context on DNA conformation in solution, *J. Mol. Biol. 314*, 423−432.
43. Eley, D. D., and Spivey, D. I. (1962) Semiconductivity of organic substances. IX. Nucleic acid in the dry state, *Trans. Faraday Soc. 58*, 411−415.

44. Porath, D., Bezryadin, A., de Vries, S., and Dekker, C. (2000) Direct measurement of electrical transport through DNA molecules, *Nature 403*, 635−638.
45. Qu, X., Trent, J. O., Fokt, I., Priebe, W., and Chaires, J. B. (2000) Allosteric, chiral-selective drug binding to DNA, *Proc. Natl. Acad. Sci. U.S.A. 97*, 12032−12037.
46. Qu, X., Wan, C., Becker, H.-C., Zhong, D., and Zewail, A. H. (2001) The anticancer drug−DNA complex: Femtosecond primary dynamics for anthracycline antibiotics function, *Proc. Natl. Acad. Sci. U.S.A. 98*, 14212−14217.
47. Gewirtz, D. A. (1999) A critical evaluation of the mechanisms of action proposed for the antitumor effects of the anthracycline antibiotics adriamycin and daunorubicin, *Biochem. Pharmacol. 57*, 727−741.
48. Oliveira-Brett, A. M., Vivan, M., Fernandes, I. R., and Piedade, J. A. P. (2002) Electrochemical detection of in situ adriamycin oxidative damage to DNA, *Talanta 56*, 959−970.
49. Chu, X., Shen, G. L., Jiang, J. H., Kang, T. F., Xiong, B., and Yu, R. Q. (1998) Voltammetric studies of the interaction of daunomycin anticancer drug with DNA and analytical applications, *Anal. Chim. Acta 373*, 29−38.
50. Pang, D. W., Zhang, M., Wang, Z. L., Qi, Y. P., Cheng, J. K., and Liu, Z. Y. (1996) Modification of glassy carbon and gold electrodes with DNA, *J. Electroanal. Chem. 403*, 183−188.
51. Leng, F. F., Savkur, R., Fokt, I., Przewloka, T., Priebe, W., and Chaires, J. B. (1996) Base Specific and regioselective chemical Cross-Linking of daunorubicin to DNA, *J. Am. Chem. Soc. 118*, 4731−4737.
52. Szulawska, A., Gniazdowski, M., and Czyz, M. (2005) Sequence specificity of formaldehyde-mediated covalent binding of anthracycline derivatives to DNA, *Biochem. Pharmacol. 69*, 7−18.
53. Yang, X. L., and Wang, A. H. J. (1999) Structure studies of atom-specific anticancer drugs acting on DNA, *Pharmacol. Ther. 83*, 181−215.
54. Zhang, H., Yu, H., Ren, J., and Qu, X. (2006) Reversible B-Z DNA transition under the low salt condition and non-B form polydApolydT selectivity by a cubane-like europium-L-aspartic acid complex, *Biophys. J. 90*, 3203−3207.
55. Zhang, H., Yu, H., Ren, J., and Qu, X. (2006) PolydA and polyrA self-structured by a europium and amino acid complex, *FEBS Lett. 580*, 3726−3730.
56. Mergny, J. L., and Lacroix, L. (2003) Analysis of thermal melting curves, *Oligonucleotides 13*, 515−537.
57. Qu, X., Chou, J., Lu, T., Dong, S., Zhou, C., and Cotton, T. M. (1995) Promoter effect of halogen anions on the direct electrochemical reaction of cytochrome c at gold electrodes, *J. Electroanal. Chem. 381*, 81−85.
58. Qu, X., Lu, T., Dong, S., Zhou, C., and Cotton, T. M. (1994) Electrochemical reaction of cytochrome c at gold electrodes modified with thiophen containing one functional group, *Bioelectrochem. Bioenerg. 34*, 153−156.
59. Vasiliskov, V. A., Prokopenko, D. V., and Mirzabekov, A. D. (2001) Parallel multiplex thermodynamic analysis of coaxial base stacking in DNA duplex by oligodeoxyribonucleotide microchips, *Nucleic Acids Res. 29*, 2303−2313.
60. Yakovchuk, P., Protozanova, E., and Frank-Kamenetskii, M. D. (2006) Base-stacking and base-pairing contributions into thermal stability of the DNA double helix, *Nucleic Acids Res. 34*, 564−574.
61. Roll, C., Ketterle, C., Faibis, V., Fazakerley, G. V., and Boulard, Y. (1998) Conformations of nicked and gapped DNA structures by NMR and molecular dynamic simulations in water, *Biochemistry 37*, 4059−4070.
62. Benight, A. S., Gallo, F. J., Paner, T. M., Bishop, K. D., Faldasz, B. D., and Lane, M. J. (1995) *Advances in Biophysical Chemistry*, Vol. 5, pp 1−55, JAI Press Inc., Greenwich, CT.
63. Qu, X., and Chaires, J. B. (2000) Analysis of drug−DNA binding data, *Methods Enzymol. 321*, 353−369.
64. Sarapuu, A., Vaik, K., Schiffrin, D. J., and Tammeveski, K. (2003) Electrochemical reduction of oxygen on anthraquinone-modified glassy carbon electrodes in alkaline solution, *J. Electroanal. Chem. 541*, 23−29.
65. Bard, A. J., and Faulkner, L. R. (2001) *Electrochemical Methods: Fundamentals and Applications*, 2nd ed., Wiley & Sons, New York.
66. Laviron, E. (1979) General Expression of the Linear Potential Sweep Voltammogram in the case of Diffusionless Electrochemical Systems, *J. Electroanal. Chem. 101*, 19−28.
67. Napper, A. M., Liu, H. Y., and Waldeck, D. H. (2001) The nature of electronic coupling between ferrocene and gold through alkanethiolate monolayers on electrodes: The importance of chain composition, interchain coupling, and quantum interference, *J. Phys. Chem. B 105*, 7699−7707.
68. Wang, J., Ozsoz, M., Cai, X. H., Rivas, G., Shiraishi, H., Grant, D. H., Chicharro, M., Fernandes, J., and Palecek, E. (1998) Interactions of antitumor drug daunomycin with DNA in solution and at the surface, *Bioelectrochem. Bioenerg. 45*, 33−40.

BI061103I